Brazilian Journal of Physics (2018) 48:130–136
https://doi.org/10.1007/s13538-018-0558-8

SOCIEDADE BRASILEIRA DE FÍSICA

CONDENSED MATTER

Self-Assembled CNT-Polymer Hybrids in Single-Walled Carbon Nanotubes Dispersed Aqueous Triblock Copolymer Solutions

D. Vijayaraghavan[1] · A. S. Manjunatha[1] · C. G. Poojitha[1]

Received: 27 September 2017 / Published online: 26 February 2018

Abstract
We have carried out scanning electron microscopy (SEM), differential scanning calorimetry (DSC), small angle X-ray scattering (SAXS), electrical conductivity, and ^{1}H NMR studies as a function of temperature on single-walled carbon nanotubes (SWCNTs) dispersed aqueous triblock copolymer (P123) solutions. The single-walled carbon nanotubes in this system aggregate to form bundles, and the bundles aggregate to form net-like structures. Depending on the temperature and phases of the polymer, this system exhibits three different self-assembled CNT-polymer hybrids. We find CNT-unimer hybrid at low temperatures, CNT-micelle hybrid at intermediate temperatures wherein the polymer micelles are adsorbed in the pores of the CNT nets, and another type of CNT-micelle hybrid at high temperatures wherein the polymer micelles are adsorbed on the surface of the CNT bundles. Our DSC thermogram showed two peaks related to these structural changes in the CNT-polymer hybrids. Temperature dependence of the ^{1}H NMR chemical shifts of the molecular groups of the polymer and the AC electrical conductivity of the composite also showed discontinuous changes at the temperatures at which the CNT-polymer hybrid's structural changes are seen. Interestingly, for a higher CNT concentration (0.5 wt.%) in the system, the aggregated polymer micelles adsorbed on the CNTs exhibit cone-like and cube-like morphologies at the intermediate and at high temperatures respectively.

Keywords Carbon nanotube · Cnt-poymer hybrid · SEM · ^{1}H NMR · Self-assembly · Electrical conductivity

1 Introduction

Block copolymers in aqueous solution are used to disperse carbon nanostructures like carbon black nanoparticles [1], fullerenes [2], and carbon nanotubes [3–5]. Block copolymers incorporated with magnetite nanoparticles are used in controlled drug-targeting delivery [6]. It is suggested that the end-functionalized block copolymer-coated carbon nanotubes can be manipulated and placed in a desired location on a surface which will be useful in many technological applications [7]. Considering the importance of the nanostructure-polymer system, it is essential to understand the interaction between the constituents. The amphiphilic block copolymers poly (ethylene oxide)-poly (propylene oxide)-poly (ethylene oxide) $PEO_yPPO_xPEO_y$ or Pluronic block copolymers self-assemble in water into micelles consisting of hydrophobic PPO core and solvated PEO corona [8]. Though the dispersion of colloidal particles like carbon black in polymer solution do not affect the self-assembly of polymer molecules and the structure of the formed micelles, the dispersion of carbon nanotubes in polymer solution is found to modify the temperature, enthalpy, and dynamic behavior of polymer self-assembly [8]. Florent et al. studied the self-assembly and aggregation of block copolymers in dispersion of single-walled carbon nanotubes by spin probe electron paramagnetic resonance (EPR) spectroscopy [9]. They reported that in the presence of dispersed SWCNTs, self-assembly and aggregation of polymer molecules occur on the nanotube and result in the formation of a new type of hybrid SWNT-polymer nanostructure. It is seen that in these systems, free polymer micelles do not form and aggregation takes place on the surface of the dispersed SWNT, and these aggregates are larger than those formed in the native solutions of pluronics [9].

Amphiphilic block copolymers are excellent dispersants for SWCNTs in aqueous environments, where their noncovalent attachments do not alter the structural, electronic, and mechanical properties of the tubes [10]. The stabilization of the SWCNTs is due to the hydrophobic blocks being

✉ D. Vijayaraghavan
vijay@rri.res.in

[1] Raman Research Institute, Sadashivanagar, Bangalore 560 080, India

attached to the nanotube surface, and the hydrophilic blocks emanate into the solvent, creating an entropic (steric) repulsion between the tubes [10]. The strength of the repulsion increases with increasing the length of the PEO chains and surface coverage [11]. For short PEO chain lengths (< 100), polymers tethered at low surface coverage present a rather weak repulsion [11]. Nativ-Roth et al. obtained a stable dispersion of 0.1 wt.% SWCNT in 0.15 wt.% of F127 in water, and the HRTEM image of the diluted dispersion with a polymer concentration of 0.035 wt.% on drying showed individual nanotubes [12]. We are interested to study the SWCNT dispersions of P123 polymer in water wherein the number of PO units is the same as F127 (70 units), but the number of EO units (20 units) is smaller with respect to that of F127 (106 units). We obtained a stable SWCNT dispersion in 2.5 wt.% of P123 in water for two different SWCNT concentrations, namely, 0.25 and 0.5 wt.%. We analyzed these samples using scanning electron microscopy (SEM), differential scanning calorimetry (DSC), small angle X-ray scattering (SAXS), electrical conductivity, and ^{1}H NMR studies as a function of temperature. Depending on the temperature and phases of the polymer, this system exhibits three different self-assembled CNT-polymer hybrids. We find CNT-unimer hybrid at low temperatures, CNT-micelle hybrid at intermediate temperatures wherein the polymer micelles are adsorbed in the pores of the CNT nets, and another type of CNT-micelle hybrid at high temperatures wherein the polymer micelles are adsorbed on the surface of the CNT bundles. Interestingly, for a higher CNT concentration (0.5 wt.%) in the system, the aggregated polymer micelles adsorbed on the CNTs exhibit cone-like and cube-like morphologies at the intermediate and at high temperatures respectively.

2 Experimental

A PEO-PPO-PEO block copolymer, pluronic P123 and deuterium oxide (99.9%), and 2,2-dimethyl-2-silapentane-5-sulfonate sodium salt (DSS) were purchased from Sigma-Aldrich and used without further purification. Single-walled carbon nanotubes (P2-SWCNT) were purchased from Carbon Solutions, Inc. (USA), and used as it is. Pluronic P123 has a molecular weight of 5800 and PEO content of 30%. On the basis of the molecular weight and chemical composition, P123 can be represented by $EO_{20}PO_{70}EO_{20}$. An aqueous 2.5 wt.% of P123 was prepared by dissolving 34 mg of P123 in 1.3 g of D_2O. This solution was stirred and sonicated for 10 min for uniform mixing. A stock solution of 0.6 M DSS in D_2O was prepared. For ^{1}H NMR measurements, a 2-μl stock solution of DSS is added to 1.2 ml of aqueous polymer solution for calibration purposes. The solution was sonicated for 10 min and then transferred to a 5-mm NMR sample tube and stored in a refrigerator before use. For the preparation of the CNT-polymer composites, appropriate amounts of SWCNTs were added to the aqueous polymer solution containing DSS, and the composite is stirred and sonicated for 15 min for uniform mixing and a uniform black solution indicating a homogeneous dispersion of CNTs in the polymer solution was obtained. The CNT containing polymer solutions was transferred to the 5-mm NMR sample tubes and stored in the refrigerator. ^{1}H NMR measurements were carried out on a 500 MHz Bruker Avance spectrometer. Sample temperatures were varied using a Bruker variable temperature accessory (AH 0020). NMR data was collected in the heating cycle starting from 20 °C after the sample reaches the equilibrated desired temperature. For scanning electron microscopy (SEM) study, for specific stable temperatures, a small portion of P123/water/SWCNT sample was transferred to a solid substrate (indium tin oxide-coated glass plate) and dried in an oven (about 60 °C), and SEM images were taken at room temperature using Carl Zeiss SMT ULTRA plus scanning electron microscope (Germany). DSC studies were carried out on this sample from 16 to 50 °C by varying the sample temperature at the rate of 1 °C/min using a Perkin-Elmer DSC-7 instrument under N_2 gas flow. NMR, SEM, and DSC experiments were repeated to ascertain reproducible results. For SAXS studies, the sample was filled in a glass capillary of 1-mm diameter and flame sealed. The sample temperature was controlled using a computer-controlled temperature controller.

The diffraction data was collected while heating the sample (0.5 °C/min). The details of the experimental setup for SAXS measurements were given elsewhere [13, 14]. AC electrical conductivity measurements were carried out using a conductivity meter PC Testr 35 (Eutech Instruments, Singapore) while heating the sample. For conductivity measurements, the CNT/polymer/water systems were prepared using deionized (Millipore) water.

3 Results and Discussion

Figure 1 shows the SAXS pattern of 0.25 wt.% SWCNTs dispersed in aqueous (D_2O) solution containing 2.5 wt.% P123 at two different temperatures 25 and 45 °C (Fig. 1a, b, respectively). The SAXS pattern exhibits peaks in the ratio $1:\sqrt{3}:2:\sqrt{7}$ indicating a 2D hexagonal structure similar to the SAXS pattern reported for SWCNT bundles [15, 16]. This indicates that in our P123/CNT/D_2O system, the dispersed single-walled carbon nanotubes exist as bundles. We find that these CNT bundles aggregate to form net-like structures (Fig. 2). The SAXS peaks shift marginally towards higher q values at higher temperature (Fig. 1b). We believe that this may be due to some marginal changes in the hexagonal ordering of the nanotubes forming bundles at higher temperatures.

Figure 2 shows the SEM images of 0.25 wt.% (Fig. 2a–c) and 0.5 wt.% (Fig. 2d–f) single-walled carbon nanotubes

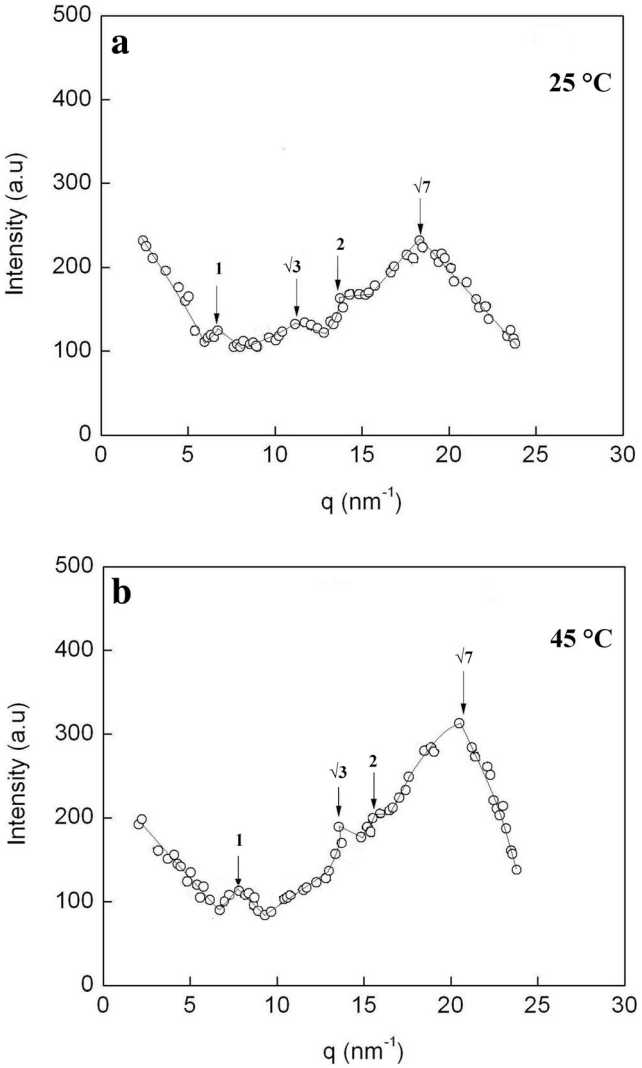

Fig. 1 SAXS pattern of 0.25 wt.% SWCNTs dispersed aqueous (D_2O) solution containing 2.5 wt.% P123 at two different temperatures (25 and 45 °C). The SAXS pattern exhibits peaks in the ratio 1:√3:2:√7 indicating a 2D hexagonal structure similar to the SAXS pattern reported for SWCNT bundles

dispersed aqueous (D_2O) solution containing 2.5 wt.% P123 as a function of temperature (the temperatures of the samples are specified in the figure). Net-like CNT structures are seen in the images. We find some bright spherical regions or domains (of 25 nm diameter) in the images. We attribute this to the aggregated polymer molecules associated with the CNT nanostructures. We believe that the observed domains at low temperatures (Fig. 2a, d) are related to the adsorbed P123 unimers (2.5 wt.% P123 in D_2O exhibits unimer to micellar transition at 20 °C as seen from our DSC data). They are mostly adsorbed in the pores of the CNT net-like structures. We attribute the bright domains at intermediate and high temperatures (Fig. 2b, c) to the adsorbed P123 micelles. At intermediate temperatures, the micelles are adsorbed in the pores of CNT net (Fig. 2b). However, at high temperatures, the micelles are adsorbed on the outer surface of the CNT bundles (Fig. 2c). We also find that increasing the temperature results in a decrease in the packing of the CNT bundles or loosening of the CNT net-like structure (Fig. 2a–c). In the case of 0.5 wt.% CNT, the images exhibit cone-like (Fig. 2e) and cube-like (Fig. 2f) morphologies associated with CNT nets. We believe that these cone-like and cube-like structures are due to the aggregation/self-assembly of the polymer micelles in the system. The polymer cones seem to emerge from the pores of the CNT net-like structure (Fig. 2e), resulting in a flower-like pattern (Fig. 2e) whereas the polymer cubes seem to be adsorbed on the surface of the nanotube bundles (Fig. 2f). In general, the average bundle diameter of the CNTs decreases with increasing temperature. For 0.25 wt.% CNT, the average bundle diameters are 12 and 9 nm at 17 and 50 °C, respectively. For 0.5 wt.% CNT, the average bundle diameters are 17 and 6 nm at 17 and 50 °C respectively. It is known that above the critical micellar temperature (CMT), dense adsorption of polymer molecules occurs on the CNT surface [17]. This may lead to an increase in the repulsion between the nanotubes at higher temperatures resulting in a decrease in the SWCNT bundle diameter.

Figure 3a shows the DSC thermogram on heating for the native polymer solution (2.5 wt.% P123 in D_2O). The thermogram exhibits an exothermic peak at 20 °C. We believe that the peak is related to the unimer to micellar phase transition of the polymer. Figure 3b shows the DSC thermogram on heating for 0.25 wt.% SWCNT dispersed polymer solution. The thermogram exhibits two exothermic peaks, one at 20 °C and another at 45 °C. We believe that the peaks are related to the structural changes in the CNT-polymer hybrids in the system. The low-temperature peak is related to the transition of the CNT-unimer hybrid to the CNT-micelle hybrid wherein the micelles are adsorbed in the pores of the CNT net-like structures and the high-temperature peak is related to the transition of the CNT-micelle hybrid to another type of CNT-micelle hybrid wherein the micelles adsorbed on the surface of the CNT bundles. Briefly, using our SEM and DSC results, we infer that this P123/D_2O/SWCNT system, depending on the temperature and phases of the polymer, exhibits three different CNT-polymer hybrids. Below 20 °C, the system exhibits a CNT-unimer hybrid. In the temperature range 20 to 45 °C, it exhibits a CNT-micelle hybrid, and above 45 °C, it exhibits another type of CNT-micelle hybrid.

Figure 4a, b shows the ^{1}H NMR spectra for an aqueous (D_2O) solution containing 2.5 wt.% P123 as a function of temperature. The NMR spectra corresponding to the PO-CH_3 groups of the polymer are shown in Fig. 4b. The peak corresponding to the PO-CH_3 groups occur near 1.1 ppm. With increasing temperature, the peak shifts upfield. The NMR spectra corresponding to the EO-CH_2 and PO-CH_2 groups of the polymer are shown in Fig. 4a. A sharp peak at about 3.7 ppm is seen which is attributed to the protons of EO-

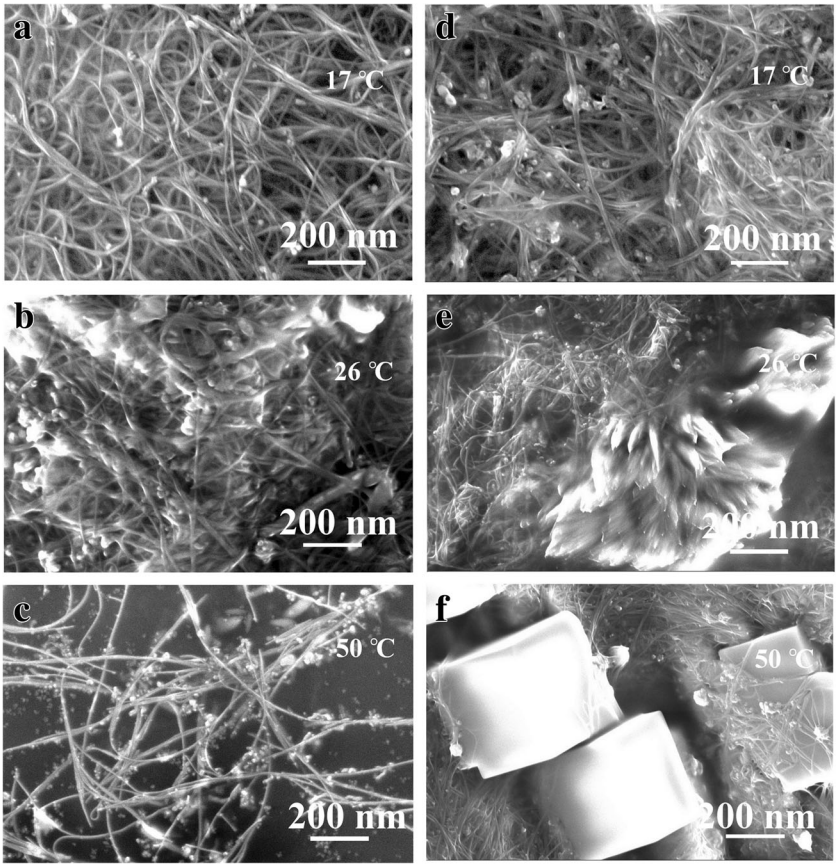

Fig. 2 SEM images of SWCNTs dispersed aqueous (D_2O) solution containing 2.5 wt.% P123 as a function of temperature for 0.25 wt.% CNTs (**a**–**c**) and 0.5 wt.% CNTs (**d**–**f**). At low temperatures (below CMT), the polymer unimers are adsorbed in the pores of the net-like structures of the CNT bundles (**a**, **d**). At intermediate temperatures (above CMT), the polymer micelles are adsorbed in the pores of the CNT structures (**b**, **e**). At higher temperatures, the micelles are adsorbed on the surface of the CNT bundles. For a higher CNT concentration (0.5 wt.%) in the system, the polymer micelles adsorbed on the CNTs aggregate to form cone-like and cube-like morphologies at the intermediate and at high temperatures, respectively (**e**, **f**). CNT bundle diameter decreases with increasing the temperature of the system

CH_2 groups remain unchanged with increasing temperature. The observed broad peaks with clearly visible hyperfine structure (from 3.6 to 2.9 ppm) come from the PO-CH_2 groups. The observed ^{1}H NMR spectrum agrees well with that reported for P123 in D_2O [18]. With increasing temperature, the PO-CH_2 peaks do not change until the micellization temperature (20 °C) is reached. At this temperature, the peaks change drastically, the hyperfine structure disappears, the line width of the peaks increases, and one of the peaks shifts towards the lower parts per million values. Similar ^{1}H NMR spectra are reported for 1 wt.% F127 in D_2O by Wanka et al. [19]. They reasoned that the PO groups are transferred on micellization from the aqueous medium into the hydrophobic micellar core, and due to the aggregation process, they have a reduced mobility which results in the broadening of the PO peaks. However, most of the EO groups remain at the micellar surface and in contact with the solvent water.

Figure 4c, d shows the NMR spectra for 0.25 wt.% SWCNTs dispersed polymer solution as a function of temperature. All the peaks are found to be very broad with respect to the NMR peaks observed for the native solution. We believe that this may be due to the formation of CNT-polymer hybrids in the CNT dispersed solution as seen in our SEM images. This indicates that the molecular groups of the polymer are adsorbed on the CNT surface resulting in their reduced mobility. The sharp EO-CH_2 peak seen in the native solution is also found to be broad in the CNT dispersed solution. This indicates that the EO-CH_2 groups of the polymer micelles which are in contact with water in the native solution may also be adsorbed on the CNT surface in the CNT dispersed solution. This will reduce the free movement of the EO chains resulting in the observed broadening of the NMR peaks.

Figure 4e, f shows the NMR spectra for 0.5 wt.% SWCNTs dispersed polymer solution as a function of temperature. Again, we find that all the peaks are very broad with respect to the NMR peaks observed for the native solution. Interestingly, at higher temperatures (above 22 °C), the peaks are found to become sharper. The sharpening of the peaks at higher temperatures may be related to the cone-like and cube-like ordering of polymer micelles as seen in our SEM images. It is not clear at this stage the reason behind the observation of ordered polymer structures adsorbed on the CNT nets when the CNT concentration in the polymer solution is high. It is reported that under the influence of surface pressure, the micelles of block copolymers exhibit different morphologies/structures, namely, spherical, cylindrical, and planar/lamellar [20–22]. We believe that increasing the CNT concentration in the micellar solution increases the surface pressure on the micelles in the vicinity of the CNT structures and the resulting aggregation of the micelles leads to the observed cone-like

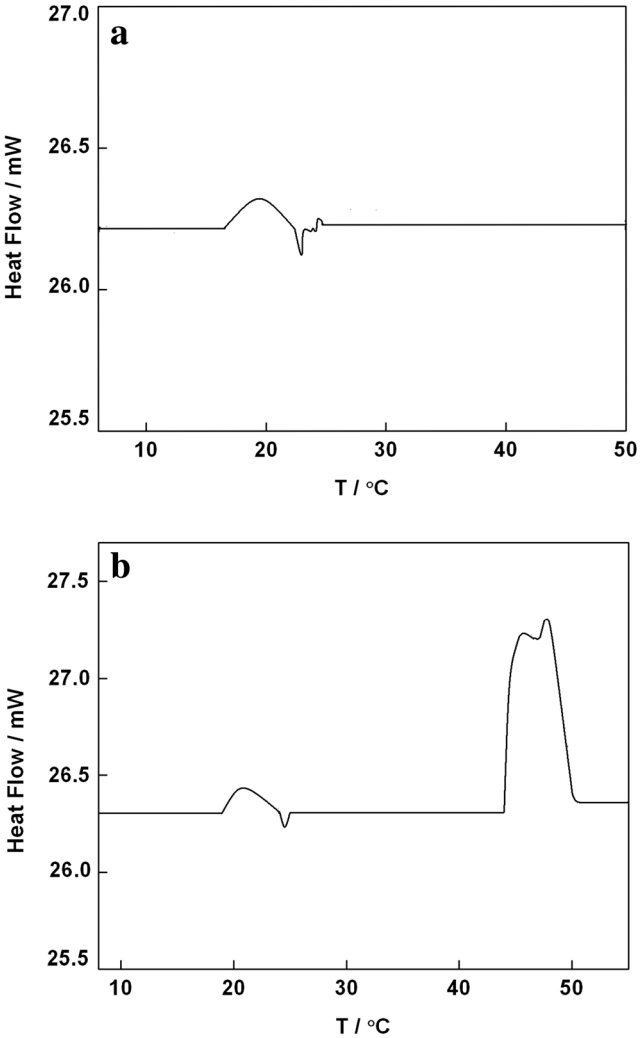

Fig. 3 **a** DSC thermogram on heating for the native polymer solution (2.5 wt.% P123 in D_2O). The thermogram exhibits an exothermic peak at 20 °C. We believe that the peak is related to the unimer to micellar phase transition of the polymer. **b** DSC thermogram on heating for 0.25 wt.% SWCNTs dispersed polymer solution. The thermogram exhibits two exothermic peaks, one at 20 °C and another at 45 °C. We believe that the peaks are related to the structural changes in the CNT-polymer hybrids in the system. The low-temperature peak is related to the transition of the CNT-unimer hybrid to CNT-micelle hybrid wherein the micelles are adsorbed in the pores of the CNT net-like structures, and the high-temperature peak is related to the transition of the CNT-micelle hybrid to another CNT-micelle hybrid wherein the micelles adsorbed on the surface of the CNT bundles

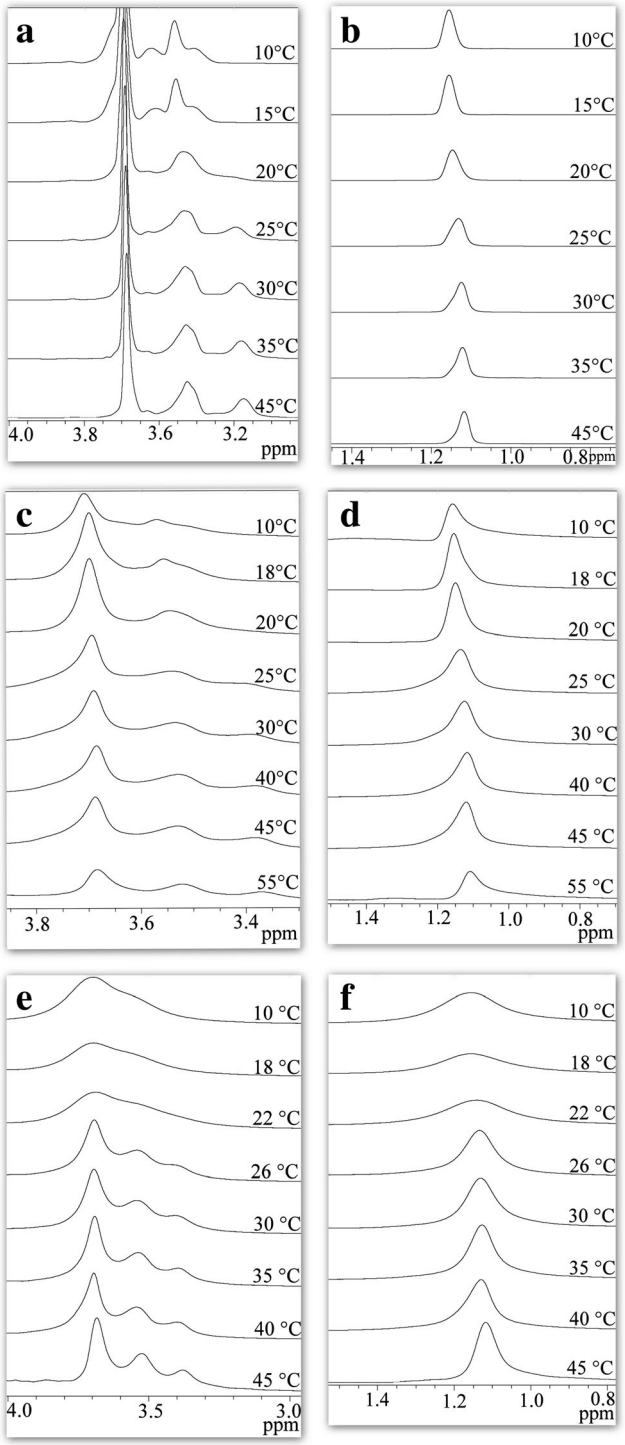

Fig. 4 ^{1}H NMR spectra for SWCNTs dispersed aqueous (D_2O) solution containing 2.5 wt.% P123 as a function of temperature for 0 wt.% (**a**, **b**), 0.25 wt.% (**c**, **d**), and 0.5 wt.% CNTs (**e**, **f**). The spectra corresponding to the PO-CH_3 groups of the polymer are shown in the **b**, **d**, **f**. The spectra corresponding to the EO-CH_2 and PO-CH_2 groups of the polymer are shown in **a**, **c**, **e**

and cube-like polymer structures adsorbed on the CNT nets. However, more studies are required to ascertain this inference.

Figure 5a, b shows the temperature-dependent chemical shifts of the PO-CH_3 signals of 0.25 and 0.5 wt.% SWCNTs dispersed polymer solutions respectively. We find discontinuous changes in the chemical shifts at 20 °C and about 45 °C. We believe that the discontinuous changes are related to the CNT-polymer hybrid structural changes.

Figure 6 shows the Arrhenius plots for native polymer solutions. From the slopes of the linear region of the Arrhenius plot, the activation energy for the conduction process is determined. The ln(σ) versus 1000/T plot for the native polymer solution shows a discontinuous change at the critical micellar

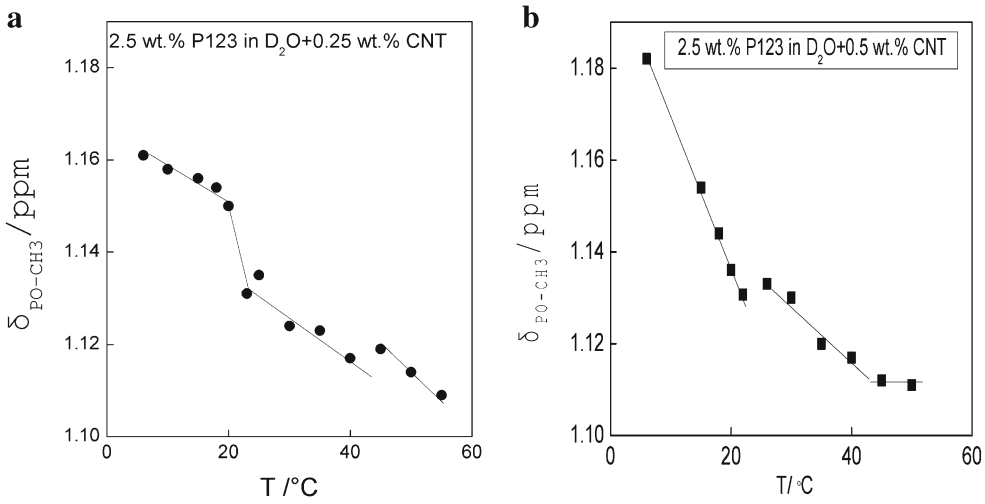

Fig. 5 Temperature-dependent chemical shifts of the PO-CH_3 signals of **a** 0.25 wt.% and **b** 0.5 wt.% SWCNTs dispersed polymer solution. We find discontinuous changes in the chemical shifts at 20 °C and about 45 °C. We believe that the discontinuous changes are related to the CNT-polymer hybrid's structural changes

temperature (CMT). The activation energies for conduction in the unimer and micellar phases of the polymer are 15.6 and 10.5 kJ/mol, respectively. Interestingly, the observed activation energy for the P123 (nonionic) micelles is found to be in the same order of magnitude of the nonionic micelles like Brij-35 and TX-100 micelles reported earlier [23]. In the case of CNT dispersed polymer solution, the ln(σ) versus 1000/T plot show discontinuous changes at the temperatures at which the observed structural changes of CNT-polymer hybrids are seen (Fig. 7). The high-temperature CNT-micellar hybrid the activation energy (~ 10 kJ/mol) is similar to that of the free micelles observed in the native polymer solution. However, the activation energies of CNT-unimer hybrids at low temperatures and CNT-micelle hybrids at intermediate temperatures are relatively smaller. We believe that this may be related to the nature of adsorption of the polymer molecules in the CNT nets. The polymer molecules are adsorbed in the pores of the CNT nets in the low and intermediate temperatures while they are adsorbed on the surface of the CNT bundles at high temperatures as seen in our SEM images.

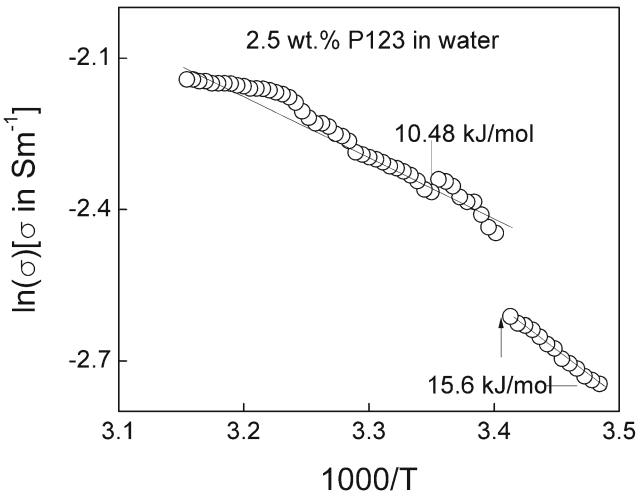

Fig. 6 Arrhenius plot for AC electrical conductivity (σ) for the native polymer solution (2.5 wt.% P123 in water). The plot shows a discontinuous change at the critical micellar temperature (CMT). From the slopes of the linear regions of the plot, the activation energy for the conduction process is determined. The calculated activation energies are also shown in the figure

4 Conclusions

We have carried out scanning electron microscopy (SEM), differential scanning calorimetry (DSC), small angle X-ray

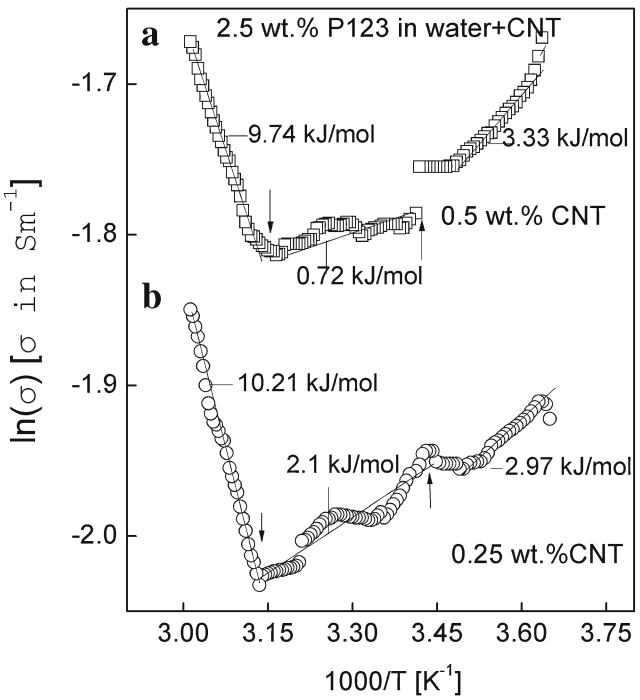

Fig. 7 Arrhenius plots for AC electrical conductivity (σ) for 0.25 and 0.5 wt% SWCNTs dispersed in aqueous triblock copolymer solution. The plots show discontinuous changes at the temperatures at which the structural changes of the CNT-polymer hybrid is observed. The calculated activation energies for conduction in each of the CNT-polymer hybrids are also shown in the figure

scattering (SAXS), electrical conductivity, and ^{1}H NMR studies as a function of temperature on single-walled carbon nanotubes (SWCNTs) containing aqueous triblock copolymer (P123) solutions. The single-walled carbon nanotubes in this system aggregate to form bundles, and the bundles aggregate to form net-like structures. Depending on the temperature and phases of the polymer, we find that this system exhibits three different self-assembled CNT-polymer hybrids. Temperature dependence of the ^{1}H NMR chemical shifts of the molecular groups of the polymer and the AC electrical conductivity of the composite also showed discontinuous changes at the temperatures at which the CNT-polymer hybrid's structural changes are seen. Interestingly, for a higher CNT concentration (0.5 wt.%) in the system, the aggregated polymer micelles adsorbed on the CNTs exhibit cone-like and cube-like morphologies.

Acknowledgements The authors would like to thank K.N. Vasudha for DSC measurements and A. Dhason for SEM images. The authors (ASM and CGP) thank the Raman Research Institute for the VSP fellowship.

References

1. Y. Lin, P. Alexandridis, Temperature dependent adsorption of pluronic F127 block copolymers onto carbon black particles dispersed in aqueous media. J. Phys. Chem. B **106**, 10834–10844 (2002)
2. N. Aich, L.K. Boateng, J.R.V. Flora, N.B. Saleh, Preparation of non-aggregating aqueous fullerenes in highly saline solutions with biocompatible non-ionic polymer. Nanotechnology **24**, 395602 (2013)
3. G. Ciofani, V. Raffa, V. Pensabene, A. Menciassi, P. Daripo, Dispersion of multi-walled carbon nanotubes in aqueous pluronic F127 solutions for biological applications. Fullerenes Nanotubes Carbon Nanostruct. **17**, 11–25 (2009)
4. I. Szleifer, R. Yerushalmi-Rozen, Polymers and carbon nanotubes-dimensionality. Interactions Nanotechnol. **46**, 7803–7818 (2005)
5. R. Yerushalmi-Rozen, I. Szleifer, Utilizing polymers for shaping the interfacial behavior of carbon nanotubes. Softmatter **2**, 24–28 (2006)
6. S. Chen, Y. Li, C. Guo, J. Wang, J. Ma, X. Liang, L. Yang, H. Liu, Temperature-responsive magnetite/PEO-PPO-PEO block copolymer nanoparticles for controlled drug targeting delivery. Langmuir **23**, 12669–12676 (2007)
7. R. Nap, I. Szleifer, Control of carbon nanotube-surface interactions: the role of grafted polymers. Langmuir **21**, 12072–12075 (2005)
8. R. Shvartzman-Cohen, M. Florent, D. Goldfarb, I. Szleifer, R. Yerushalmi-Rozen, Aggregation and self-assembly of amphiphilic block copolymers in aqueous dispersions of carbon nanotubes. Langmuir **24**, 4625–4632 (2008)
9. M. Florent, R. Shvartzman-Cohen, D. Goldfarb, R. Yerushalmi-Rozen, Self-assembly of pluronic copolymers in aqueous dispersions of single-wall carbon nanotubes as observed by spin probe EPR. Langmuir **24**, 3773–3779 (2008)
10. R. Shvartzman-Cohen, Y. Levi-Kalisman, E. Nativ-Roth, R. Yerushalmi-Rozen, Generic approach for dispersing single-walled carbon nanotubes: the strength of a weak interaction. Langmuir **20**, 6085–6088 (2004)
11. R. Shvartzman- Cohen, E. Nativ-Roth, E. Baskaran, Y. Levi-Kalisman, I. Szleifer, R. Yerushalmi-Rozen, Selective dispersion of single-walled carbon nanotubes in the presence of polymers: the role of molecular and colloidal length scales. J. Am. Chem. Soc **126**, 14850–14857 (2004)
12. E. Nativ-Roth, R. Shvartzman- Cohen, C. Bounioux, M. Florent, D. Zhang, I. Szleifer, R. Yerushalmi-Rozen, Physical adsorption of block copolymers to SWNT and MWNT: a nonwrapping mechanism. Macromolecules **40**, 3676–3685 (2007)
13. D. Vijayaraghavan, Self-assembled ordering of single-walled carbon nanotubes in a lyotropic liquid crystal system. J. Mol. Liq. **199**, 128–132 (2014)
14. D. Vijayaraghavan, Self-assembled superlattices of gold nanoparticles in a discotic liquid crystal. Mol. Cryst. Liq. Cryst. **508**, 101–114 (2009)
15. P. Launois, A. Marucci, B. Vigolo, P. Bernier, A. Derre, P. Poulin, Structural characterization of nanotube fibers by X-ray scattering. J. Nanosci. Nanotech. **1**, 125–128 (2001)
16. D. Vijayaraghavan, Aggregates of single-walled carbon nanotube bundles in a surfactant solution. J. Mol. Liq. **209**, 440–446 (2015)
17. M. Granite, A. Radulescu, W. Pyckhout-Hintzen, Y. Cohen, Interactions between block copolymers and single-walled carbon nanotubes in aqueous solutions: a small angle neutron scattering study. Langmuir **27**, 751–759 (2011)
18. J. Ma, C. Guo, Y. Tang, J. Wang, L. Zheng, X. Liang, S. Chen, H. Liu, Microenvironmental and conformational structure of triblock copolymers in aqueous solution by ^{1}H and ^{13}C NMR spectroscopy. J. Colloid Interface Sci. **299**, 953–961 (2006)
19. G. Wanka, H. Hoffmann, W. Ulbricht, Phase diagrams and aggregation behavior of poly(oxyethylene)-poly(oxypropylene)-poly(oxyethylene) triblock copolymers in aqueous solutions. Macromolecules **27**, 4145–4159 (1994)
20. J. Zhu, R.B. Lennox, A. Eisenberg, Polymorphism of (quasi) two-dimensional micelles. J. Phys. Chem. **96**, 4727–4730 (1992)
21. D.J. Meier, *In thermoplastic elastomers, Eds* (Hanser, Newyork, 1987) Chapter 11
22. S. Li, S. Hanley, I. Khan, S.K. Varshney, A. Eisenberg, R.B. Lennox, Surface micelle formation at the air/water interface from nonionic diblock copolymers. Langmuir **9**, 2243–2246 (1993)
23. D. Vijayaraghavan, Magnetic susceptibility and electrical conductivity studies on the aqueous solutions of two nonionic surfactants. J. Mol. Liq. **166**, 76–80 (2012)